Journal of Cell Science 113, 1365-1372 (2000)
Printed in Great Britain © The Company of Biologists Limited 2000
JCS1072



# Selective permeability of different connexin channels to the second messenger inositol 1,4,5-trisphosphate

**Heiner Niessen[1], Hartmann Harz[2], Peter Bedner[1], Karsten Krämer[1] and Klaus Willecke[1,*]**

[1]Institut für Genetik, Abt. Molekulargenetik, Universität Bonn, Römerstr. 164, 53117 Bonn, Germany
[2]Botanisches Institut, Ludwig-Maximilians-Universität, Menzinger Straße 67, 80638 München, Germany
*Author for correspondence (e-mail: genetik@uni-bonn.de)

*Accepted 13 February; published on WWW 21 March 2000*

## SUMMARY

**Intercellular propagation of signals through connexin32-containing gap junctions is of major importance in physiological processes like nerve activity-dependent glucose mobilization in liver parenchymal cells and enzyme secretion from pancreatic acinar cells. In these cells, as in other organs, more than one type of connexin is expressed. We hypothesized that different permeabilities towards second messenger molecules could be one of the reasons for connexin diversity. In order to investigate this, we analyzed transmission of inositol 1,4,5-trisphosphate-mediated calcium waves in FURA-2-loaded monolayers of human HeLa cells expressing murine connexin26, -32 or -43. Gap junction-mediated cell coupling in different connexin-transfected HeLa cells was standardized by measuring the spreading of microinjected $Mn^{2+}$ that led to local quenching of FURA-2 fluorescence. Microinjection of inositol 1,4,5-trisphosphate into confluently growing HeLa connexin32 transfectants induced propagation of a $Ca^{2+}$ wave from the injected cell to neighboring cells that was at least three- to fourfold more efficient than in HeLa Cx26 cells and about 2.5-fold more efficient than in HeLa Cx43 transfectants. Our results support the notion that diffusion of inositol 1,4,5-trisphosphate through connexin32-containing gap junctions is essential for the optimal physiological response, for example by recruiting liver parenchymal cells that contain subthreshold levels of this short lived second messenger.**

Key words: Connexin26, Connexin32, Connexin43, Gap junction, $Ca^{2+}$ imaging, FURA-2, Non-regenerating $Ca^{2+}$ wave

## INTRODUCTION

At least 15 different connexin genes exist in the mouse genome, coding for subunit proteins of gap junction channels (Bruzzone et al., 1996; Condorelli et al., 1998; Soehl et al., 1998; Manthey et al., 1999). It is not known how far this diversity of connexin channels reflects an adaptation to specific exchange of metabolites between cells. In particular, second messengers like inositol 1,4,5-trisphosphate ($IP_3$) or cyclic nucleotides are possible mediators of intercellular signalling, since they have been shown to act as long-range messengers in single cells (Allbritton et al., 1992; Kasai et al., 1994). Here we have studied the role of $IP_3$ in gap junction-mediated intercellular signalling through defined connexin channels.

Microinjection studies with rat hepatocytes previously demonstrated that hepatic gap junctions are permeable to $IP_3$ (Sàez et al., 1989). Furthermore, in vitro studies of glucose mobilization from glycogen in primary rat hepatocytes showed that the glycogenolytic effect of vasopressin was reduced by 70%, after total supression of cell coupling with common gap junction blockers (Eugenin et al., 1998). However, these studies did not investigate whether each of the different connexin channels present in hepatocytes contributes equally to this effect. Double whole-cell patch-clamp experiments revealed that gap junction channels of cultured primary hepatocytes consisted of homotypic Cx32 and Cx26 channels as well as heterotypic Cx26/Cx32 channels (Valiunas et al., 1999). Mice deficient in Cx32 showed a decreased ability to mobilize glucose from hepatic glycogen, although some cell coupling was still found, due to the remaining Cx26 channels (Nelles et al., 1996; Stümpel et al., 1998). Both studies attributed the decreased glucose mobilization to diminished gap junctional intercellular communication by $IP_3$.

This second messenger appears in the cytoplasm after stimulation of certain G-protein coupled receptors which, in turn, activate phospholipase C. This enzyme hydrolyzes phosphatidylinositol 4,5-bisphosphate to $IP_3$ and diacylglycerol. $IP_3$ subsequently binds to intracellular receptor channels on membranes of the endoplasmatic reticulum, which release $Ca^{2+}$ ions from intracellular stores into the cytoplasm (Berridge and Irvine, 1989; Berridge, 1997).

This signal transduction process might also be involved in synchronous contraction of vascular smooth muscles, where gap junction channels consisting of Cx43 are possible candidates for mediating intercellular signaling. Endothelial cells and vascular smooth muscle cells show expression of Cx43 and Cx40, whereas Cx37 is additionally expressed in most endothelial cells (Christ et al., 1992). Carter et al. (1996) showed that Cx43 channels were permeable to photolabile derivatives of $IP_3$ (caged $IP_3$). Endocrine and paracrine signals reach the tissues of

vascular wall either from autonomous nerve endings at the adventitial border or via blood circulation from the endothelial side. Therefore gap junction-mediated cell coupling could be crucial for signal propagation during smooth muscle contraction.

In order to investigate whether different connexin channels show different permeabilities towards $IP_3$, we have compared $Ca^{2+}$ wave propagation after injection of $IP_3$ into human HeLa cells transfected with murine Cx26, -32 or -43. This heterologous expression system offers the possibility of selecting stable transfectants against a very low background of endogenous connexin proteins (Cao et al., 1998) and allows analysis of only one type of connexin channel (Elfgang et al., 1995). Furthermore, $IP_3$-induced $Ca^{2+}$ release is well documented in HeLa cells (Bootman et al., 1994, 1997) and has been shown to be similar to that in liver parenchymal cells (Hajnóczky and Thomas, 1997; Rooney et al., 1989).

## MATERIALS AND METHODS

### Cell culture

HeLa wild-type cells were cultured in Dulbecco's modified Eagle medium supplemented with 10% fetal calf serum (Gibco), 100 i.u./ml penicillin and 100 μg/ml streptomycin (Sigma, Deisenhofen, Germany) (standard medium). Connexin-transfectants (Elfgang et al., 1995) were cultured in standard medium supplemented with 1 μg/ml puromycin (Sigma). Cultures were kept in plastic vessels (Falcon) in an incubator at 37°C under an atmosphere of 10% $CO_2$.

Prior to fluorometric $[Ca^{2+}]_i$ measurements, cells were plated on glass coverslips, which were placed into a 35 mm plastic Petri dish. Cells were grown for 60-85 hours and used for experiments after reaching a confluence of 80-90%.

#### Coculture

HeLa wild-type cells were plated on a 35 mm plastic dish and grown to confluency. Then cells were incubated with isotonic glucose solution containing 10 μg/ml DiI (Molecular Probes, Eugene, USA) for 15 minutes at 37°C. After being washed twice with phosphate-buffered saline (PBS), the DiI-labeled HeLa wild-type cells and HeLa connexin transfectants were trypsin treated, centrifuged and resuspended. DiI-labeled cells were mixed with unlabeled cells at a ratio of 1:25, plated onto glass coverslips and grown for 48-72 hours prior to microinjection experiments.

### Microinjection and electrophysiology

Microelectrodes were pulled from borosilicate glass capillaries (Hilgenberg, Malsfeld, Germany) with a horizontal pipette puller (Sutter Instruments Inc., Eugene, USA) and filled with 100 mM KCl, 10 mM Hepes, pH 7.2, containing either 1 mM inositol 1,4,5-trisphosphate (Molecular Probes) or 50 mM $MnCl_2$. Microelectrode resistance was 240-260 MΩ for $IP_3$ injections and 40-50 MΩ for $MnCl_2$ injections. Impaling was performed with an electronic micromanipulator (Eppendorf, Hamburg, Germany). Membrane potentials were measured with an intracellular amplifier/filter unit (Heinecke, Seewiesen, Germany) and displayed on a two-channel digital oscilloscope (Tektronics, Köln, Germany). $IP_3$ was iontophoretically applied with a constant current of 5 nA over a period of 30 seconds, unless otherwise stated. $MnCl_2$ solution was injected by hydrostatic pressure of the microelectrode over a period of 150 seconds. Microelectrodes for $MnCl_2$ injections were discarded after each injection and when resistance was below 40 or higher than 55 MΩ.

Neurobiotin (N-2[aminoethyl]-biotinamide hydrochloride; Vector Laboratories, Burlingame, CA, USA; 6% w/v) and rhodamine B isothiocyanate dextran (0.4% w/v) were iontophoretically injected for 2-4 seconds in 0.1 M Tris buffer, pH 7.6, using a positive current of 20 nA. 5 minutes after injection, cells were washed twice with PBS, fixed for 10 minutes in 1% glutaraldehyde in PBS without $Ca^{2+}$ and $Mg^{2+}$, pH 7.4, washed twice with PBS, incubated in 0.4% Triton X-100, washed with PBS, incubated with horseradish peroxidase-avidin D (Vector Laboratories) for 2.5 hours, washed with PBS, and incubated in 0.05% diaminobenzidine 0.003% hydrogen peroxide solution for another 15-20 minutes.

### Fluorometric measurements

Cells were loaded with 5 μM FURA-2/AM (Molecular Probes) and 0.025% PLURONIC F-127 in Hepes-buffered saline (HBS) containing 140 mM NaCl, 5 mM KCl, 2 mM $CaCl_2$, 1 mM $MgCl_2$, 10 mM Hepes and 10 mM glucose, pH 7.4 ($HBS^+$) for 45 minutes at room temperature. After loading, cells were rinsed with HBS without addition of $CaCl_2$ ($HBS^-$), the coverslip was transferred to the experimental chamber, filled with 500 μl $HBS^-$ containing 100 μM BAPTA-dextrane and 100 μM suramin, and mounted onto an inverse epifluorescence microscope (Axiovert 100, Zeiss Oberkochen, Germany). Fluorescence measurements were performed using a commercial imaging system (T.I.L.L. Photonics, Planegg, Germany) consisting of a high-performance grating monochromator and a 12 bit-charged coupled-device camera connected to a personal computer (Messler et al., 1996). All CCD-images were background-corrected by subtraction of a dark picture. The product of light intensity, measured with a UV-sensitive photodiode, and exposure time were held constant to ensure identical light exposition of frames for each experiment. Cell populations that differed more than 25% from the mean value in FURA-2 fluorescence were discarded.

For $Mn^{2+}$ diffusion measurements, 31 full frames were recorded at a wavelength of 360 nm with a frequency of 0.1 Hz. Injection was performed after the first frame. The steady decline in mean fluorescence of the full frame during the injection period was taken as proof for continuous contact of injection pipette and cytoplasm of the injected cell. Cells with complete quenching of FURA-2 fluorescence were chosen to measure background fluorescence. Mean fluorescence of the first frame and 150 seconds after $Mn^{2+}$ injection were background corrected and used to calculate the decrease in mean fluorescence.

For $[Ca^{2+}]_i$ measurements, FURA-2 fluorescence was monitored at 340/380 nm excitation wavelength. Impaling of the cell was performed under the control of $[Ca^{2+}]_i$. In about 50% of the cases, impaling led to an increase in $[Ca^{2+}]_i$ in the impaled cell and occasionally this excitation spread to neighboring cells as well. Injections were performed only after the complete return of $[Ca^{2+}]_i$ to baseline levels. 180 frames were recorded at a frequency of 1 Hz, with 5 frames preceding the injection. Absolute $Ca^{2+}$ concentrations were calculated using the method of Grynkiewicz et al. (1985). $R_{min}$ and $F380_{min}$ were determined by iontophoretic injection of EGTA (pipette concentration: 25 mM) into the cytoplasm of several cells. $R_{max}$ and $F380_{max}$ were subsequently determined by perfusing the cells with $HBS^+$ containing 2.5 μM ionomycin and 20 mM $Ca^{2+}$.

Results of $Mn^{2+}$ quench measurements and $Ca^{2+}$ wave propagation were analyzed for statistical significance using the Mann-Whitney test.

## RESULTS

### Connexin-transfected HeLa cells show intercellular propagation of $Ca^{2+}$ waves after $IP_3$ injection

$IP_3$-induced $Ca^{2+}$ release was used as an indicator of intercellular $IP_3$ diffusion. Saturating amounts of $IP_3$ were injected iontophoretically for 30 seconds with a current of 5 nA into one cell of a confluent layer of HeLa cells. The cytoplasmic $Ca^{2+}$ concentration ($[Ca^{2+}]_i$) was quantified for 180 seconds in an area of 220×164 μm using the $Ca^{2+}$ indicator FURA-2. Injections were carried out in $Ca^{2+}$-free Hepes-buffered salt solution in

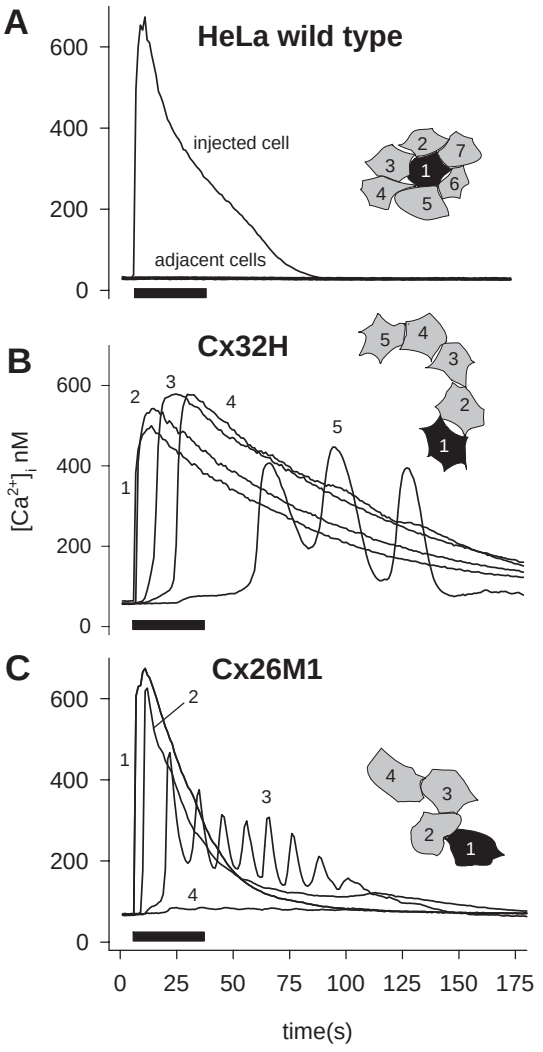


**Fig. 1.** $IP_3$ injections into HeLa cells in $Ca^{2+}$-free extracellular buffer. $[Ca^{2+}]_i$ is plotted over time for the injected cell and several adjacent cells, as indicated in the cartoons. (A) Injection of $IP_3$ into Hela wild-type cells resulted in an increase in $[Ca^{2+}]_i$ to more than 500 nM, which remained restricted to the injected cell. (B) After $IP_3$ injection, Cx32-transfected HeLa cells showed an increase in $[Ca^{2+}]_i$ in the injected cell, which propagated to adjacent cells up to the 4$^{th}$ order. (C) Cx26-transfected HeLa cells displayed responses to $IP_3$ injection similar to Cx32-transfected cells, but $Ca^{2+}$ wave propagation was restricted to cells of the first and second order. In all examples $IP_3$ was injected with 5 nA current for 30 seconds, as indicated by the black bar.

order to avoid capacitive $Ca^{2+}$ entry through $Ca^{2+}$ store-operated $Ca^{2+}$ channels. Cells were used for experimentation for up to 1 hour. During this time $[Ca^{2+}]_i$ remained stable and cells remained attached to the coverslip. To reduce the participation of secreted ATP to $Ca^{2+}$ wave propagation, 100 μM suramin was added to the extracellular medium.

Fig. 1 shows the changes in intracellular $Ca^{2+}$ concentration during injection of $IP_3$ for HeLa wild-type, Cx32- and Cx26-transfected HeLa cell clones. $IP_3$ injection into confluently growing HeLa wild-type cells resulted in a strong increase of $[Ca^{2+}]_i$ in the injected cell but not in adjacent cells (Fig. 1A). In contrast, injections into Cx32-transfected HeLa cells led to an increase in $[Ca^{2+}]_i$ in neighboring cells up to the fourth order (Fig. 1B). In Fig. 1C, HeLa Cx26 (clone M1)-transfected cells responded to $IP_3$ injection with an increase in $[Ca^{2+}]_i$ in cells of the first order and one cell of the second order. In all connexin-transfected HeLa cells tested, the $Ca^{2+}$ wave propagation stopped at cell boundaries and usually proceeded only after a latency period of 1-10 seconds at the site of contact. Frequently, the starting point of the intracellular $Ca^{2+}$ wave could not be clearly determined, because the regenerative $Ca^{2+}$ release was preceded by a smaller and homogenous increase in $[Ca^{2+}]_i$ throughout the cytoplasm. Oscillations in $[Ca^{2+}]_i$ of varying frequency could be observed in all connexin-transfected cells at the periphery of the $Ca^{2+}$ wave (see Fig. 1B, no. 5 and C, no. 3).

The $[Ca^{2+}]_i$ increase in neighboring HeLa-Cx26 cells could still be observed when $Ca^{2+}$ stores of the cell injected with $IP_3$ had been depleted by injections of low current. Fig. 2A shows the effect of subsequent short injections of $IP_3$ with a current of 1nA, which resulted in a progressive depletion of intracellular $Ca^{2+}$ stores until no further $[Ca^{2+}]_i$ increase was observed. The following $IP_3$ injection of 5 nA and 30 seconds duration resulted in an intercellular $Ca^{2+}$ wave spreading over three cells, although the increase in $[Ca^{2+}]_i$ in the injected cell remained below those in adjacent cells. No backflow of $Ca^{2+}$ ions could be observed (Fig. 2). The same results were obtained for Cx32- and Cx43-transfected HeLa cells.

Injection of pipette buffer without addition of $IP_3$ elicited no propagating $Ca^{2+}$ wave in HeLa wild-type and connexin-transfected HeLa cells ($n$=14, data not shown).

In order to determine whether diffusion of extracellular factors contributed to the observed $Ca^{2+}$ wave propagation induced by injection of $IP_3$, we labeled HeLa wild-type cells with the lipophilic membrane marker DiI and plated them together with Cx32-transfected HeLa cells (clone H). HeLa wild-type cells were accordingly distinguished from HeLa-Cx32 cells by the red fluorescence of DiI, which showed only minor spectral overlap with the indicator dye FURA-2. DiI-labeled HeLa cells exhibited no difference in response to extracellular stimulation with 5 μM ATP (data not shown). $IP_3$ injection into a Cx32-transfected HeLa cell, in close apposition to HeLa wild-type cells, resulted in $Ca^{2+}$ wave propagation in Cx32-transfected HeLa cells but not in HeLa wild-type cells ($n$=8, Fig. 3).

### Gap junctional intercellular communication can be evaluated by measuring the spreading of microinjected $Mn^{2+}$ ions in confluently growing HeLa-connexin transfectants

Comparison of $IP_3$ diffusion in HeLa clones expressing different connexins requires information about the relative number of functional gap junction channels between these cells. In cell pairs, junctional coupling is usually deduced from measurements of electrical conductance and determined by double whole-cell patch-clamp experiments. However, electrophysiological measurements are difficult to interpret in a system where many cells are electrically coupled. Therefore, the extent of intercellular diffusion of $Mn^{2+}$ ions was used to determine the relative coupling levels in different HeLa connexin transfectants. We took advantage of the quenching effect of $Mn^{2+}$ ions on FURA-2 fluorescence and its high affinity to $Mn^{2+}$ ($K_d$=2.8 nM; Kwan et al., 1990). Frames for $Mn^{2+}$ quench experiments were recorded with 360 nm

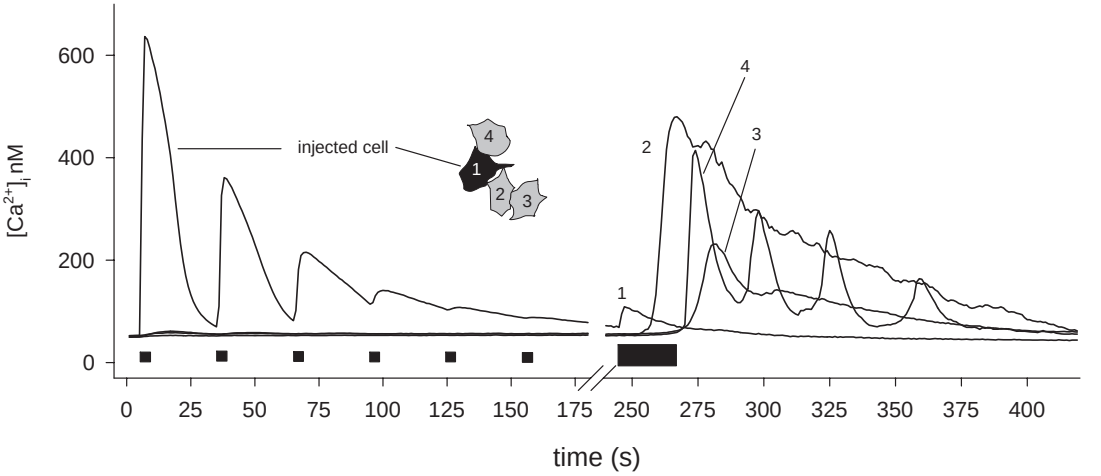


**Fig. 2.** $Ca^{2+}$ release in neighboring cells could still be observed when $Ca^{2+}$ stores of the injected cell had been depleted by preceeding injections of low current. One cell of confluently growing Cx26-transfected HeLa cells was periodically injected with $IP_3$, as indicated by the black bars (1 nA, 5 seconds). The resulting $Ca^{2+}$ transient decreased in amplitude to undetectable levels after five injections. Subsequent $IP_3$ injection into the same cell with 5nA current and 30 seconds duration resulted in a $[Ca^{2+}]_i$ increase in three adjacent cells. The relative positions of the cells are indicated in the cartoon.

excitation light, which excluded fluorescence fluctuations due to changes in $[Ca^{2+}]_i$.

In order to reduce the influence of different FURA-2 concentrations on results of $Mn^{2+}$ quenching experiments, we used only similarly loaded cell populations. No correlation between dye concentration and the relative decrease in mean fluorescence could be detected in all $Mn^{2+}$ injections performed ($n$=114; data not shown).

Four different HeLa cell clones transfected with Cx26, -32 and -43 were used: Cx26C, Cx26M1, Cx32H, Cx43K7. Injections of $Mn^{2+}$-containing solution performed with FURA-2-loaded HeLa wild-type and connexin-transfected cells are illustrated in Fig. 4. The corresponding normalized changes in fluorescence of single HeLa wild-type and HeLa Cx26M1 cells are plotted in Fig. 5A,B (positions are indicated in the cartoon). The $Mn^{2+}$ ions quenched the FURA-2 fluorescence in the injected cells within 1-3 seconds. In the following period of 180 seconds, the fluorescence decrease remained restricted to the injected cell in HeLa wild-type cells (Figs 4, 5A). In all connexin-transfected HeLa cells, in contrast, radially spreading fluorescence quenching was observed. In HeLa-Cx26M1, as illustrated in Fig. 5B, the fluorescence in cells of the fourth order was still completely quenched.

In order to compare the coupling of different HeLa clones, we quantified the spreading of microinjected $Mn^{2+}$ by the decrease of FURA-2 fluorescence. The mean fluorescence was measured prior to injection and 150 seconds after $Mn^{2+}$ injection in an area of 220×164 μm centered around the injected cell and corrected for background fluorescence. The fluorescence values were used to calculate the normalized extent of $Mn^{2+}$ diffusion. Fig. 5C shows the increase over time of the area where $Mn^{2+}$ ions quenched the Fura-2 fluorescence, for the injections presented in Fig. 4.

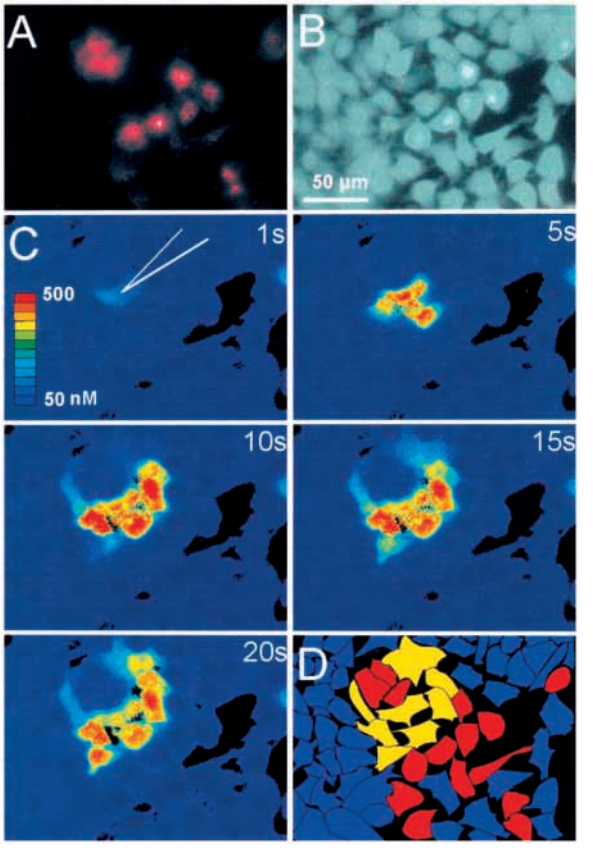


**Fig. 3.** The propagation of $Ca^{2+}$ waves was dependent on functional gap junctions between Cx32-transfected HeLa cells. (A) Monolayer of cocultured HeLa wild-type and HeLa-Cx32H cells photographed under 560 nm illumination. HeLa wild-type cells exhibited red fluorescence due to prelabeling with DiI. (B) FURA-2 fluorescence of cells in the same field, photographed under 360 nm illumination. (C) Pseudocolor representation of the $Ca^{2+}$ wave propagation in the mixed monolayer of cocultured cells during the first 20 seconds of injection. The $IP_3$-injected cell is indicated by the arrowhead. (D) Schematic representation of the mixed monolayer. HeLa wild-type cells are shown in red, responding Cx32H cells in yellow, non-responding Cx32H cells in blue color. The colour scale indicates $[Ca^{2+}]_i$.

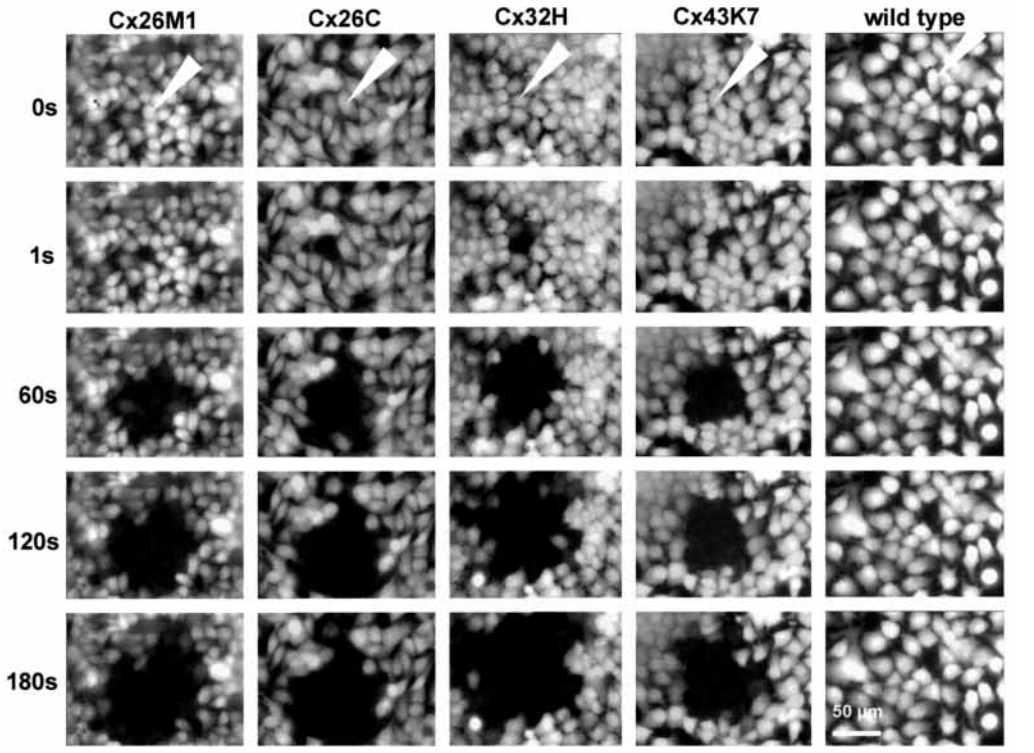


**Fig. 4.** Quenching of FURA-2 fluorescence at different times after $Mn^{2+}$ injection into HeLa wild type and different clones of HeLa cells transfected with Cx26, -32 or -43. Arrowheads point to microinjected cells. Frames were recorded with 360 nm excitation light, in order to avoid fluorescence changes due to $[Ca^{2+}]_i$ fluctuations.

The complete quenching of FURA-2 fluorescence in the injected cell corresponded to a mean area of 1876±137 $\mu m^2$ ($n$=12) and was subtracted from the normalized extent of $Mn^{2+}$ diffusion. No fluorescence decrease was observed in HeLa wild-type cells adjacent to the injected cell.

For connexin-transfected HeLa cell clones we obtained the following results: Cx26C, 6525±824 $\mu m^2$ ($n$=22); Cx26M1, 8826±793 $\mu m^2$ ($n$=21); Cx32H, 7566±784 $\mu m^2$ ($n$=26); Cx43K7, 4899±380 $\mu m^2$ ($n$=24). These results are represented by black columns in Fig. 6. The HeLa clones Cx26C and Cx26M1 showed no significant difference in $Mn^{2+}$ diffusion relative to Cx32H cells and were assumed to have a corresponding level of $Mn^{2+}$-penetrable gap junctions channels. HeLa-Cx43K7 cells showed a lower extent of $Mn^{2+}$ diffusion relative to HeLa-Cx32H cells. This difference of intercellular $Mn^{2+}$ permeability is significant ($P$<0.025).

In order to compare the relative diffusion of $Mn^{2+}$ to the spreading of neurobiotin in Cx26-, Cx32- and Cx43-transfected HeLa cells, we performed iontophoretic neurobiotin injections in addition to $Mn^{2+}$ diffusion measurements (see Materials and Methods). Experiments were performed on different HeLa cell clones transfected with the same connexins. Fig. 7 shows similar ratios of neurobiotin spreading and $Mn^{2+}$ diffusion for different connexin-transfected clones, indicating that both methods of standardization gave similar results.

### Different HeLa-connexin transfectants showed distinct propagation of $Ca^{2+}$ waves after $IP_3$ injections

In order to compare the permeability of different gap junction channels to $IP_3$, we injected this compound into one cell of a confluent monolayer as described above. The number of cells that showed an increase in $[Ca^{2+}]_i$ up to 250 nM during 180 seconds after injection was taken as a measure for intercellular propagation of the $Ca^{2+}$ wave. 20-25 injections of $IP_3$ were performed for each HeLa clone. $IP_3$ injection into individual HeLa-Cx32H cells of a confluent monolayer resulted in propagation of the $Ca^{2+}$ wave to an average of 17±7 cells. The $Ca^{2+}$ wave spread throughout all neighboring cells of the first order and always reached cells of the second order. In 19 of 27 injections, even cells of the third and fourth order participated in the $Ca^{2+}$ wave. In contrast, $IP_3$ injections into HeLa-Cx26C cells led to regenerative $Ca^{2+}$ release in only 4±2 of the adjacent cells. Only 9 of 27 $IP_3$ injections resulted in a $Ca^{2+}$ wave reaching second order cells. Similar results were obtained for Cx26M1 cells, where $Ca^{2+}$ wave propagation reached an average of 6±2 cells and in 11 of 20 cases responding cells were of the second order. HeLa-Cx43K7 cells showed propagation of $Ca^{2+}$ waves to an average of 6±2 cells. Second order cells were reached in 17 of 27 cases. In HeLa wild type, 2 of 10 injections resulted in a $[Ca^{2+}]_i$ increase in one neighboring cell. This corresponded to a mean $Ca^{2+}$ wave propagation to 0.2 cells. The results for all HeLa clones tested are summarized in Fig. 6 (white bars).

## DISCUSSION

Here we have shown that injection of $IP_3$ into HeLa cells transfected with exogenous Cx26, -32 or -43 gap junctional channels resulted in a $Ca^{2+}$ wave that propagated with different efficiency into adjacent cells, depending on the specific connexin channel expressed. The strong increase in $[Ca^{2+}]_i$ to about 500 nM, observed in injected and adjacent cells, was solely dependent on intracellular $Ca^{2+}$ release, since injections were performed in $Ca^{2+}$-free extracellular medium and led to depletion of intracellular $Ca^{2+}$ stores (cf. Figs 1, 2).

Intercellular $Ca^{2+}$ wave propagation has been shown in different cell lines and primary cell cultures (Frame and de

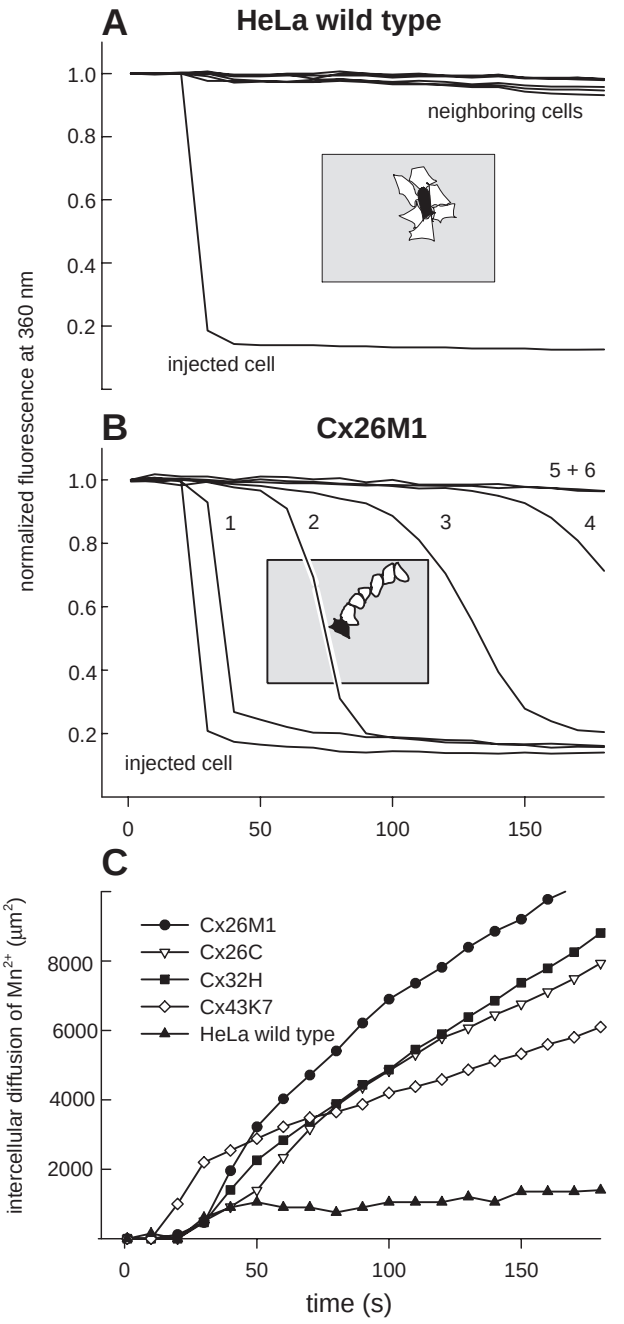


**Fig. 5.** Evaluation of fluorescence changes during $Mn^{2+}$ injection. (A,B) Normalized FURA-2 fluorescence recorded at 360 nm excitation plotted over time for single HeLa wild-type and HeLa-Cx26M1 cells. The data were taken from measurements shown in Fig. 4. Relative positions of the cells are indicated by the cartoons. (C) Calculated normalized extent of $Mn^{2+}$ diffusion within the full frames shown in Fig. 4.

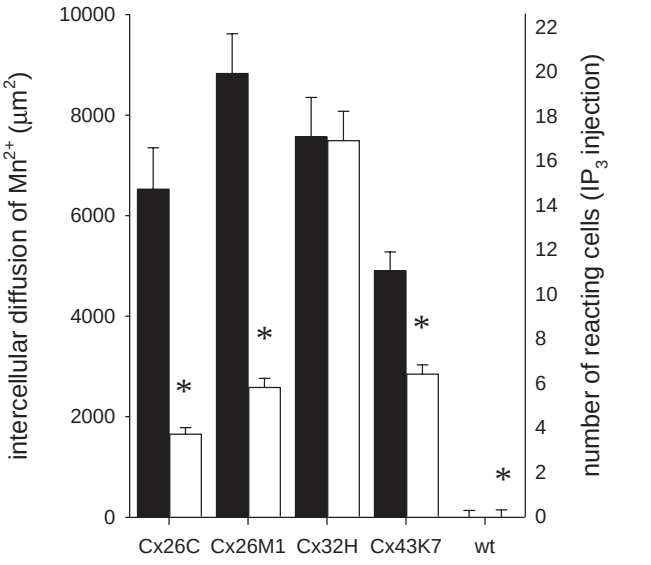


**Fig. 6.** Summarized comparison of $Mn^{2+}$-induced quenching and $IP_3$-induced $Ca^{2+}$ wave propagation in FURA-2-loaded HeLa wild type and connexin-transfected cells. Black columns: normalized extent of $Mn^{2+}$ diffusion after 150 seconds of $Mn^{2+}$ injection. HeLa transfectants: Cx26C (*n*=22), Cx26M1 (*n*=21), Cx32H (*n*=26), Cx43K7 (*n*=24); HeLa wild type (*n*=12). White columns: $IP_3$-induced $Ca^{2+}$ wave propagation (Cx26C, *n*=27; Cx26M1, *n*=20; Cx32, *n*=27, Cx43K7, *n*=27, wild type, *n*=10). All cells were counted that exhibited a $[Ca^{2+}]_i$ increase to 250 nM. Asterisks mark results that are significantly different ($P$<0.001) from that of Cx32H. Values are means ± s.e.m.

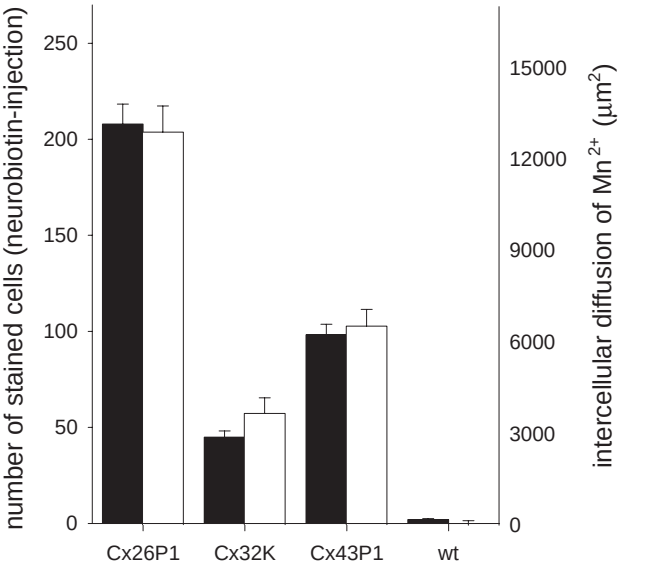


**Fig. 7.** Extent of neurobiotin or $Mn^{2+}$ diffusion in monolayers of HeLa cells transfected with Cx26, -32 as well as -43 and of HeLa wild-type cells. Experiments were performed on transfected HeLa cell clones different from those presented in Fig. 6. Black columns: extent of neurobiotin diffusion (left ordinate). HeLa transfectants: Cx26P1 (*n*=28), Cx32K (*n*=20), Cx43P1 (*n*=23); wild type (*n*=16). White columns: normalized extent of $Mn^{2+}$ diffusion (right ordinate). HeLa transfectants: Cx26P1 (*n*=20), Cx32K (*n*=20), Cx43P1 (*n*=20); wild type (*n*=7).

Feijter, 1997; Hassinger et al., 1996; Joergenson et al., 1997) including HeLa cells (Cotrina et al., 1998). However, these studies included paracrine propagation of $Ca^{2+}$ waves, resulting from diffusion of factors (probably ATP) released into the extracellular space upon mechanical stimulation of one cell in a monolayer. Therefore, we conducted several control experiments, in order to confirm that the $Ca^{2+}$ wave

propagation we studied after $IP_3$ injection was due to intercellular diffusion of $IP_3$ through gap junction channels. In our experiments we blocked any participation of released ATP by the presence of 100 μM suramin in the extracellular medium, which acted as an ATP receptor antagonist (Fredholm et al., 1994). In addition, injection of pipette buffer without $IP_3$ into connexin-transfected HeLa cells did not result in $Ca^{2+}$ wave propagation (data not shown). $IP_3$ injections into HeLa wild-type cells led to an increase of $[Ca^{2+}]_i$ in only two cases ($n$=12). Accordingly, HeLa wild-type cells did not respond with an increase in $[Ca^{2+}]_i$ after inducing a propagating $Ca^{2+}$ wave in immediately adjacent Cx32-transfected HeLa cells (Fig. 3). Massive diffusion of $Ca^{2+}$ through connexin channels was excluded, since wave propagation was still observed when $Ca^{2+}$ stores of the injected cell had been depleted before (cf. Fig. 2). This has also been confirmed for Cx32 and Cx43 transfected HeLa cells and is consistent with findings about mechanisms of $Ca^{2+}$ wave propagation in several other cell types (Sanderson et al., 1994; Yule et al., 1996). We conclude that under our experimental conditions gap junctional coupling was essential and sufficient for propagation of intercellular $Ca^{2+}$ waves in connexin-expressing HeLa cells and that $Ca^{2+}$ wave propagation was indeed based on the diffusion of $IP_3$.

### Evaluating gap junctional communication between different connexin-transfected HeLa cells by measurements of $Mn^{2+}$ diffusion

In order to determine the extent of gap junctional coupling for each connexin transfected HeLa clone, we performed diffusion measurements of $Mn^{2+}$ ions and of neurobiotin.

Although the Pauling diameter of this cation is about 0.8 Å, the $Mn^{2+}$ diffusion in monolayers of FURA-2-loaded HeLa cells transfected with connexins was slowed down due to the strong buffering effect of FURA-2 on $Mn^{2+}$ ions. The steep decrease in fluorescence of higher order cells started only after almost complete bleaching of the preceding cells. $Mn^{2+}$ diffusion measurements showed good correlation with the independently performed neurobiotin diffusion measurements performed on HeLa-Cx26M1, HeLa-Cx32K and HeLa-Cx43K7 cells, although the axial and abaxial ionic diameters of neurobiotin (5.4 and 12.7 Å) (Elfgang et al., 1995) are greater than those of $Mn^{2+}$ ions. This indicates that the molecular size of the tracer was not critical to permeability.

In contrast to the possibility of visualizing directly the diffusion of $Mn^{2+}$ in FURA-2-loaded cells, the intercellular diffusion of neurobiotin can only be evaluated after fixation of cells. Thus, this procedure precludes any dynamic measurements. A disadvantage of using $Mn^{2+}$ as the reference molecule to evaluate gap junctional communication could be the selectivity of certain connexin channels, including Cx26, -32 and -43, for anions or cations, as has been described by Veenstra (1996) for rat connexins expressed in transfected N2A mouse neuroblastoma cells. This also applies to other charged tracers, including potassium and chloride ions used in electrophysiological measurements.

We conclude that evaluating levels of gap junctional communication by $Mn^{2+}$ does not allow estimation of the absolute number of functional channels expressed in HeLa connexin-transfected cells but it is a good approximation, comparable to the standardization with neurobiotin (see Fig. 7).

### Cx32 channels are more permeable to $IP_3$ than are Cx26 or Cx43 channels

Cx32-transfected HeLa cells displayed a $Ca^{2+}$ wave propagation to 17±7 cells, whereas $Ca^{2+}$ waves in two different Cx26 transfectants spread to 6±2 and 4±2 cells. These differences are statistically significant (Mann-Whitney test, $P$<0.001). $Ca^{2+}$ waves in Cx43 transfected cells reached 6±2 cells, although it has to be considered that HeLa-Cx43K7 cells displayed lower gap junctional coupling than the other transfectants ($P$<0.025). Hence, the permeability of Cx32 gap junction channels to $IP_3$ can be assumed to be about 2.8- to 4.2-fold higher compared to Cx43- and Cx26-transfected HeLa cells, respectively. However, we have to take into account that more than 80% of the responding cells in each of the HeLa-Cx26 transfectants were first order cells surrounding the injected cell. In HeLa-Cx32H cells, by contrast, 64% of the responding cells pertained to the second and third order. Since the total volume of the cells covered by the $Ca^{2+}$ wave increased with the square of the distance from its origin, $IP_3$ was considerably diluted during diffusion to higher orders of neighboring cells. $IP_3$ is degraded by cell-specific enzymes and its half life is supposed to be between 1-30 seconds in different mammalian cells (Sims and Allbritton, 1998; Wang et al., 1995). Hence, the $IP_3$ concentration is likely to decrease considerably with distance from the site of injection. After reaching the peripheral cells, the $IP_3$ concentration first had to overcome the effective treshhold mechanism, which protects the cell against accidental $Ca^{2+}$-release by low $IP_3$ concentrations (Marchant and Taylor, 1997), before it was detected. Therefore, we conclude that the deduced permeability ratios are likely to be underestimated. Regarding Cx32 and Cx26 channels, this is supported by studies of Cao et al. (1998), who analyzed the specific permeability of these connexin channels to Lucifer yellow, using the same connexin-transfected HeLa cells that have been investigated in this study. Cao et al. (1998) reported about a ninefold wider spreading of microinjected Lucifer yellow in HeLa-Cx32H cells than in HeLa-Cx26C cells. Lucifer yellow (443 Da, charge: −2) resembles $IP_3$ (417 Da, charge: −2 to −4) in molecular mass as well as charge and one could assume that $IP_3$ might display a similar permeability ratio for Cx32 versus Cx26 channels, if it were not subject to metabolic constraints.

For investigation of $IP_3$ permeability of different connexin channels, the amount of injected $IP_3$ had to be much higher than the amount sufficient to elicit regenerative $Ca^{2+}$ release in a single cell. We consider it unlikely that a single cell produces such an excess of $IP_3$ through activation of phospholipase C. This view is supported by results of Tordjmann et al. (1997), who showed that stimulating one cell of a hepatocyte doublet with a $Ca^{2+}$-mobilizing hormone was insufficient to induce $Ca^{2+}$ release in the adjacent cell. In contrast, Cx32-deficient mice showed a decreased capability to mobilize glucose from hepatic glycogen stores upon nervous or hormonal stimulation (Nelles et al., 1996; Stümpel et al., 1998). Our findings in this paper confirm the hypothesis (Nelles et al., 1996) that the lack of Cx32 channels in Cx32-deficient mouse liver will result in decreased intercellular $IP_3$ diffusion and hence in a smaller number of liver cells responding by glucose mobilization to hormonal stimulation.

Recently we have found that spreading of $IP_3$-mediated $Ca^{2+}$ waves in primary hepatocyte doublets takes place in wild-type

hepatocytes at 25-fold lower concentration of $IP_3$ than in Cx32-deficient hepatocytes (Niessen and Willecke, 2000). This result supports the notion that a major role of Cx32 may be the preferential intercellular propagation of $IP_3$-mediated signals. It is tempting to speculate that different connexin channels may have been evolved to show selective permeabilities towards short-lived second messengers and metabolites. The expression of more than one type of connexin per cell may be an additional advantage in fulfilling these requirements. Perhaps the combination of different homomeric or heteromeric connexin channels reflects an adjustment to the functional needs of different cell types.

H.N. received a stipend of the Graduiertenkolleg 'Funktionelle Proteindomänen'. This work was supported by grants of the Deutsche Forschungsgemeinschaft through SFB 284 (C1), the Deutsche Krebshilfe to K.W., and the Fonds der Chemischen Industrie to K.W. and H.H.

## REFERENCES

**Allbritton, N. L., Meyer, T. and Stryer L.** (1992). Range of messenger action of calcium ion and inositol 1,4,5-trisphosphate. *Science* **258**,1812-1815.

**Berridge, M. J. and Irvine, R. F.** (1989). Inositol phosphates and cell signalling. *Nature* **341**,197-205.

**Berridge, M. J.** (1997). Elementary and global aspects of calcium signalling. *J. Physiol.* **499**, 291-306.

**Bootman, M. D., Berridge, M. J. and Taylor, C. W.** (1992). All-or-nothing $Ca^{2+}$ mobilization from the intracellular stores of single histamine-stimulated HeLa cells. *J. Physiol.* **450**, 163-178.

**Bootman, M. D., Cheek, T. R., Moreton, R. B., Bennett, D. B. and Berridge, M. J.** (1994). Smoothly graded $Ca^{2+}$ release from inositol 1,4,5-trisphosphate-sensitive $Ca^{2+}$ stores. *J. Biol. Chem.* **269**, 24783-24791.

**Bootman, M. D., Niggli, E., Berridge, M. J. and Lipp, P.** (1997). Imaging the hierarchical $Ca^{2+}$ signalling system in HeLa cells. *J. Physiol. Lond.* **499**, 307-314.

**Bruzzone, R., White, T. W. and Paul, D. L.** (1996). Connections with connexins: the molecular basis of direct intercellular signalling. *Eur. J. Biochem.* **23**, 1-27.

**Cao, F., Eckert, R., Elfgang, C., Nitsche, J. M., Snyder, S. A., Hülser, D. F., Willecke, K. and Nicholson, B. F.** (1998). A quantitative analysis of connexin-specific permeability differences of gap junctions expressed in HeLa transfectants and Xenopus oocytes. *J. Cell Sci.* **111**, 31-43.

**Carter, T. D., Chen, X. Y., Carlile, G., Kalapothakis, E., Ogden, D. and Evans, W. H.** (1996). Porcine aortic endothelial gap junctions: identification and permeation by caged $InsP_3$. *J. Cell Sci.* **109**, 1765-1773.

**Christ, G. J., Moreno, A. P., Melman, A. and Spray, D. C.** (1992). Gap junction-mediated intercellular diffusion of $Ca^{2+}$ in cultured human corporal smooth muscle cells. *Am. J. Physiol.* **263**, C373-C383.

**Condorelli, D. F., Parenti, R., Spinella, F., Salinaro, A. T., Belluardo, N., Cardile, V. and Cicirata, F.** (1998). Cloning of a new gap junction gene (Cx36). highly expressed in mammalian brain neurons. *Eur. J. Neurosci.* **10**, 1202-1208.

**Cotrina, M. L., Lin, J. H. C., Alves-Rodrigues, A., Liu, L. J., Azmi-Ghadimi, H., Kang, J., Naus, C. C. G. and Nedergaard, M.** (1998). Connexins regulate calcium signaling by controlling ATP release. *Proc. Natl. Acad. Sci. USA* **95**, 15735-15740.

**Elfgang, C., Eckert, R., Lichtenberg-Fraté, H., Butterweck, A., Traub, O., Klein, R. A., Hülser, D. F. and Willecke K.** (1995). Specific permeability and selective formation of gap junction channels in connexin-transfected HeLa cells. *J. Cell Biol.* **129**, 805-817.

**Eugenin, E. A., Gonzàles, H., Sàez, C. A. and Sàez, J. C.** (1998). Gap junctional communication coordinates vasopressin-induced glycogenolysis in rat hepatocytes. *Am. J. Physiol.* **274**, G1109-G1116.

**Frame, M. K. and de Feijter, A. W.** (1997). Propagation of mechanically induced intercellular calcium waves via gap junctions and ATP receptors in rat liver epithelial cells. *Exp. Cell Res.* **230**, 197-207.

**Fredholm, B. B., Abbracchio, M. P., Burnstock, G., Daly, J. W., Harden, T. K., Jacobson, K. A., Leff, P. and Williams, M.** (1994). VI. Nomenclature and classification of purinoceptors. *Physiol. Rev.* **46**, 143-153.

**Grynkiewicz, G., Poenie, M. and Tsien, R. Y.** (1985). A new generation of $Ca^{2+}$ indicators with greatly improved fluorescence properties. *J. Biol. Chem.* **260**, 3440-3450.

**Hajnóczky, G. and Thomas, A. P.** (1997). Minimal requirements for calcium oscillations driven by the $IP_3$ receptor. *EMBO J.* **16**, 3533-3543.

**Hassinger, T. D., Guthrie, P. B., Atkinson, P. B., Bennett, M. V. and Kater, S. B.** (1996). An extracellular signaling component in propagation of astrocytic calcium waves. *Proc. Natl. Acad. Sci. USA* **93**, 13268-13273.

**Joergensen, N. R., Geist, S. T., Civitelli, R. and Steinberg, T. H.** (1997). ATP- and gap junction dependent intercellular calcium signalling in osteoblastic cells. *J. Cell Biol.* **139**, 497-506.

**Kasai, H. and Petersen, O. H.** (1994). Spatial dynamics of second messengers: $IP_3$ and cAMP as long range and associative messengers. *Trends Neurosci.* **17**, 95-101.

**Kwan, C. Y. and Putney Jr., C. W.** (1990). Uptake and intracellular sequestration of divalent cations in resting and methacholine-stimulated mouse lacrimal acinar cells. Dissociation by $Sr^{2+}$ and $Ba^{2+}$ of agonist-stimulated divalent cation entry from the refilling of the agonist-sensitive intracellular pool. *J. Biol. Chem.* **265**, 678-84.

**Manthey, D., Bukauskas, F., Lee, C. G., Kozak, C. A. and Willecke, K.** (1998). Molecular cloning and functional expression of the mouse gep junction gene connexin57 in human HeLa cells. *J. Biol. Chem.* **274**, 14716-14723.

**Marchant, J. S. and Taylor, C. W.** (1997). Cooperative activation of $IP_3$ receptors by sequential binding of $IP_3$ and $Ca^{2+}$ safeguards against spontaneous activity. *Curr. Biol.* **7**, 510-518.

**Messler, P., Harz, H. and Uhl, R. J.** (1996). Instrumentation for multiwavelengths excitation imaging. *J. Neurosci. Meth.* **69**, 137-147.

**Nelles, E., Bützler, C., Jung, D., Temme, A., Gabriel, H.-D., Dahl, E., Traub, O., Stümpel, F., Jungermann, K., Zielasek, J., Toyka, K. V., Dermietzel, R. and Willecke, K.** (1996). Defective propagation of signals generated by sympathetic nerve stimulation in the liver of connexin32-deficient mice. *Proc. Natl. Acad. Sci. USA* **93**, 9565-9570.

**Niessen, H. and Willecke, K.** (2000). Strongly decreased gap junctional permeability to inositol 1,4,5-trisphosphate in connexin32 deficient hepatocytes. *FEBS Lett.* **466**, 112-114.

**Rooney, T. A., Sass, E. J. and Thomas, A. P.** (1989). Characterization of cytosolic calcium oscillations induced by phenylephrine and vasopressin in single FURA-2 loaded hepatocytes. *J. Biol. Chem.* **264**, 17131-17141.

**Sàez, J. C., Connor, J. A., Spray, D. C. and Bennett, M. V.** (1989). Hepatocyte gap junctions are permeable to the second messenger inositol 1,4,5-trisphosphate, and to calcium ions. *Proc. Natl. Acad. Sci. USA* **86**, 2708-2712.

**Sanderson, M. J., Charles, A. C., Boitano, S. and Dirksen, E. R.** (1994). Mechanisms and function of intercellular calcium signalling. *Mol. Cell. Endocrinol.* **98**, 173-187.

**Sims, E. C. and Allbritton, N. L.** (1998). Metabolism of inositol 1,4,5-trisphosphate and inositol 1,3,4,5-tetrakisphosphate by the oocytes of *Xenopus laevis*. *J. Biol. Chem.* **273**, 4052-4058.

**Soehl, G., Degen J., Teubner, B. and Willecke, K.** (1998). The murine gap junction gene connexin36 is highly expressed in mouse retina and regulated during brain development. *FEBS Lett.* **428**, 27-31.

**Stümpel, F., Ott, T., Willecke, K. and Jungermann, K.** (1998). Connexin 32 gap junctions enhance stimulation of glucose output by glucagon and noradrenaline in mouse liver. *Hepatology* **28**, 1616-1620.

**Tordjmann, T., Berthon, B., Claret, M. and Combettes, L.** (1997). Coordinated intercellular calcium waves induced by noradrenaline in rat hepatocytes: dual control by gap junction permeability and agonist. *EMBO J.* **16**, 5398-5407.

**Valiunas, V., Niessen, H., Willecke, K. and Weingart, R.** (1999). Electrophysiological properties of gap junction channels in hepatocytes isolated from Cx32 deficient and wild type mice. *Pflügers Arch. – Eur. J. Physiol.* **437**, 846-856.

**Veenstra, R. D.** (1996). Size and selectivity of gap junction channels formed from different connexins. *J. Bioenerg. Biomembr.* **28**, 327-338.

**Veenstra, R. D., Wang, H.-Z., Beblo, D. A., Chilton, M. G., Harris, A. L., Beyer, E. C. and Brink, P. R.** (1995). Selectivity of connexin-specific gap junctions does not correlate with channel conductance. *Circ. Res.* **77**, 1156-1165.

**Wang, S. S. H., Alousi, A. A. and Thompson, S. H.** (1995). The lifetime of inositol 1,4,5-trisphosphate in single cells. *J. Gen. Physiol.* **105**, 149-171.

**Yule, D. A., Stuenkel, E. and Williams, J. A.** (1996). Intercellular calcium waves in rat pancreatic acini: mechanism of transmission. *Am. J. Physiol.* **271,** C1285-C1294.